Proton–Alpha-Particle Inelastic Channels at Medium Incident Energies

M. Jung, Y. Sakamoto, J. N. Suren, C. Jacquot, and L. Girardin
Centre de Recherches Nucléaires, Universite Louis Pasteur, Laboratoire de Physique Corpusculaire, Strasbourg-Cronenbourg, France

R. Schmitt
Laboratoire du Rayonnement Cosmique, Lyon, France,
and Laboratoire de Physique Corpusculaire, Strasbourg, France
(Received 10 August 1972)

We measured the cross sections of the different inelastic channels for $\alpha+p$ reactions between 135 and 155 MeV. Starting with some simple assumptions, a theoretical description of differential and absolute cross sections has been sought to be applied to some cosmic-ray studies.

INTRODUCTION

Cosmic ray d and ^{3}He are mainly produced by interaction of primary p and α particles with interstellar hydrogen and helium. Their production rate $n_s(\epsilon, \vec{r})$ at position $\vec{r}$ and energy ϵ is connected to the primary flux $n_p(\epsilon, \vec{r})$ by a relation like

$$n_s(\epsilon, \vec{r}) \simeq \sum_i \int \sigma^i_{p\to s}(\epsilon, \epsilon') n_p(\epsilon', \vec{r}) d\epsilon' ,$$

where $\sigma^i_{p\to s}$ is the differential production cross section of a fragment with energy ϵ by interaction of a primary p with an i target.

In order to study $\alpha+p$ interactions we exposed nuclear emulsions which contain hydrogen to the Orsay α beam. The nuclear emulsion technique allows measurement of absolute cross sections as well as energy distributions of emitted fragments and gives simultaneously a complete representation of the different interaction channels.

The most important information on cosmic rays is given by their energy spectrum, and it becomes necessary to have a good representation of the differential cross sections $\sigma^i_{p\to s}(\epsilon, \epsilon')$ if one wishes to be able to compare calculated and experimental spectra.

Ramaty and Lingenfelter[1] worked in such a way and, in an important study, have given a semi-empirical representation of available results from Wilson chambers and counters in order to explain cosmic ray d and ^{3}He. The most efficient formulation is certainly an analytical but simple treatment starting with simple theoretical assumptions; we have tried in this paper to find analytical formulas for the differential cross sections as functions of outgoing fragment energy.

TECHNIQUE AND EXPERIMENT

Just a rough survey of experimental technique will be given here, as well as a summary of the absolute cross sections we measured between 135 and 155 MeV. The technique has been used in our laboratory for several years in order to study α+C, N, O reactions and further details can be found in one of the previous papers.[2]

A nuclear emulsion acts simultaneously as target and detector since it registers each charged emitted prong and allows the measurement of the whole event except for a possible emitted neutron.

To identify a reaction all the different mass and charge possibilities are assumed for each emitted prong assuming target nuclei of H, C, N, O, which are the light nuclei components of nuclear emulsion. With help of a range-energy relation, energy and momentum conservation are checked for all possible reactions. To fit events with one emitted neutron the whole missing momentum is given to the neutron and the fit made only on energy conservation. In this way the method only allows an identification of reactions with, at most, one emitted neutron. This is unimportant for the aim of this work. Indeed, the only reaction with more than one emitted neutron corresponds to the total breakup of the α particle and does not contribute to formation of d, t, or ^{3}He fragments. On the other hand this reaction has a rather high threshold (around 142 MeV) and cannot give an important contribution in the energy range studied here.

The experiment has been done with Ilford K0-K5 50% emulsion stacks irradiated at 26°. Each stack was composed of seven 900-μm-thick plates. The incident energy was 155 MeV, and because the events have been measured in the whole thickness of the first plate, we have collected a set of events corresponding to an incident energy range between 135 and 155 MeV. For this experiment we limited the scanning to the first plate of each stack because, according to the energy loss of the incident beam in the second plate we would have been under the threshold of most of the reactions.

Details on the method of determining cross sec-

tions can be found in papers mentioned in Ref. 2. For the estimate of the errors we took into account all the uncertainties introduced by scanning efficiency, incident flux, and number of target nuclei, but we note that the most important factor comes from the statistical error due to the number of identified events.

ANALYSIS OF DIFFERENTIAL CROSS SECTIONS

Before going through the different $\alpha+p$ reaction channels, let us first make some general comments.

The differential cross sections for n particles in the final state are of the form

$$d\sigma=\frac{(2\pi)^4}{\hbar v_0}|M|^2\prod_{f=1}^{n}\frac{dk_f}{(2\pi)^3}\times\delta\left(\vec{k}_0-\sum_{f=1}^{n}\vec{k}_f\right)\delta\left(E_0-\sum_{f=1}^{n}E_f\right),$$

where M is the transition matrix element between the initial and the final state and

$$M=\langle\Psi_f|V|\Psi_i\rangle.$$

The analysis will depend on the choice of wave functions for the interacting particles as well as on the potential. If the center-of-mass motion is described by a plane wave, we can write

$$\psi_{\vec{k}}(\vec{r})=Ne^{i\vec{k}\cdot\vec{r}}\phi(|\vec{r}|).$$

The radial parts for ^{3}He and α particle are chosen as a Gaussian form

$$\phi_{^3\mathrm{He}}(r)=N_{^3\mathrm{He}}\exp\left[-\frac{\alpha'}{2}\sum_{i>j=1}^{3}(\vec{r}_i-\vec{r}_j)^2\right],$$

$$\phi_\alpha(r)=N_\alpha\exp\left[-\frac{\alpha}{2}\sum_{i>j=1}^{4}(\vec{r}_i-\vec{r}_j)^2\right],$$

with[3]

$$\alpha=0.1455\times 197.3289^2\ (\mathrm{MeV}/c)^2,$$

$$\alpha'=0.1474\times 197.3289^2\ (\mathrm{MeV}/c)^2.$$

The radial part of the deuteron wave function is chosen either as the Hulthén type or the Gaussian form. The form is only related to the normalization of the theoretical results. For the Hulthén form

$$\phi_d(r)=\frac{N_d}{r}(e^{-ar}-e^{-br})$$

we used the following parameters (Ref. 3):

$$a=0.232\times 197.3289\ (\mathrm{MeV}/c);$$

$$b=1.202\times 197.3289\ (\mathrm{MeV}/c).$$

In the following part of this section we will give only the relations necessary to make clear the comparison between experiment and theory. All details can be found in the Appendixes which summarize kinematical constraints and the differential cross sections for d, t, ^{3}He emitted fragments for $p+\alpha$ and $\alpha+p$ reactions. We also want to make clear that we do not try to find a standard normalization for all the theoretical curves, but that we wish only to be able to compare the shape of theoretical and experimental distributions to see if most of the experiment can or cannot be explained by the analysis.

A. Two-Particle Final State: $\alpha+p\rightarrow d+{}^3$He

This reaction has a rather high cross section at the studied energy so that it is chosen for a somewhat more complete analysis of the contribution of the one- and two-particle transfer mechanisms. Calculations are done with the coordinates shown in Fig. 1.

1. One-Particle Transfer Mechanism

An interaction between only two nucleons takes part in the reaction. The interaction potential can be assumed to have a zero range:

$$V(\vec{r}_1-\vec{r}_5)=V_0\delta(\vec{r}_1-\vec{r}_5).$$

Even if the potential has a finite range, it is possible to eliminate it in the matrix element by solving the Schrödinger equation for the deuteron. In this case the expression $V(\vec{r}_1-\vec{r}_5)\phi_d(\vec{r}_1-\vec{r}_5)$ is replaced by the second derivative of the deuteron wave function.

Regardless of the potential form, the differential cross section for ^{3}He becomes

$$\frac{d\sigma_1}{dE_{^3\mathrm{He}}}=\frac{C}{k_0^2}\exp\left[-\frac{1}{3\alpha}\left(\vec{k}_{^3\mathrm{He}}-\frac{3\vec{k}_0}{4}\right)^2\right],$$

where $C=0.514C_V$ and k_0 is the incident momentum. Here C_V depends only on the units.

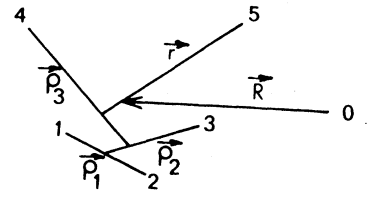

FIG. 1. Coordinate system. $\vec{R}$ is the center-of-mass position of the five particles. $\vec{r}, \vec{\rho}_1, \vec{\rho}_2, \vec{\rho}_3$ are relative coordinates.

2. Two-Particle Transfer Mechanism

Here the target proton interacts with two particles in helium to make ^{3}He. An harmonic-oscillator potential is considered:

$$V(\vec{r}) = A[(\vec{r}_1 - \vec{r}_2)^2 + (\vec{r}_1 - \vec{r}_3)^2] .$$

The constant A is expressed in terms of the parameter α' for the wave function of ^{3}He, by inserting the potential into the Schrödinger equation for the wave function. The energy distribution is

$$\frac{d\sigma_2}{dE_{^3\mathrm{He}}} = \frac{C}{k_0^2}\left[\frac{12(\alpha+\alpha')}{3\alpha'+4\alpha} - \frac{k_{^3\mathrm{He}}^2}{18\alpha'}\right]^2 \times \exp\left(-\frac{1}{4\alpha}\left|\vec{k}_{^3\mathrm{He}} - \tfrac{1}{2}\vec{k}_0\right|^2 - \frac{1}{18\alpha'}k_{^3\mathrm{He}}^2\right),$$

where $C = 68.8 C_V$.

Near threshold it is possible to assume a superposition of one- and two-particle transfer mechanisms, while at high energy one-particle transfer should certainly be sufficient. For both contributions the matrix element becomes $|M_{12}| = |M_1 + M_2|$, and the cross section can be deduced from the two preceding relations.

The energy distribution for ^{3}He is plotted in Fig. 2 with the two theoretical values: curves (1) and (2), respectively, correspond to $d\sigma_1/dE_{^3\mathrm{He}}$ and $d\sigma_{12}/dE_{^3\mathrm{He}}$.

As our incident energy range is rather broad (slightly broader than that which is used to give the absolute cross section) the theoretical calculation is made for each event and all contributions to the different emitted energy channels added. Normalizations of theoretical curves are done according to the total number of events (this allow us to drop constant C_V). From Fig. 2 it can be concluded that in a first approximation the one-particle transfer reaction explains the greater pa

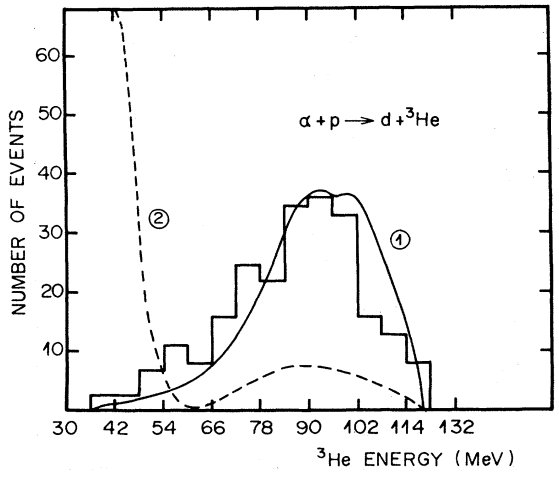

FIG. 2. $d\sigma/dE_{^3\mathrm{He}}$ for the reaction $\alpha + p \rightarrow d + {}^3$He. Experimental and theoretical distributions: (1) one-particle transfer mechanism; (2) one- plus-two-particle transfer mechanism.

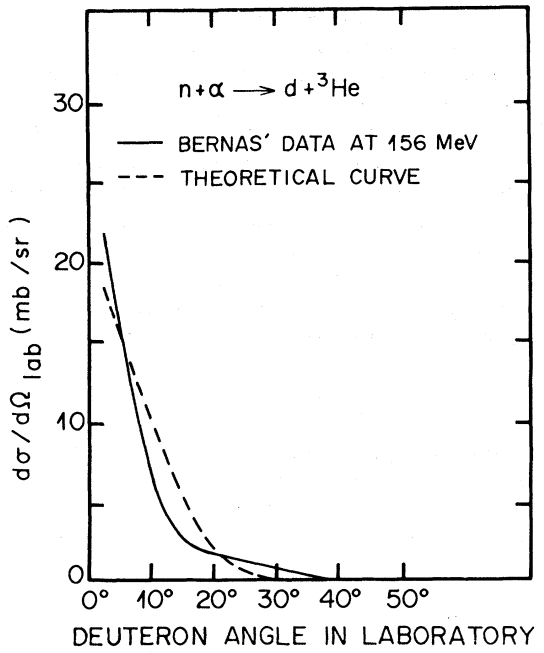

FIG. 3. $d\sigma/d\theta_{d\,\mathrm{lab}}$ for the reaction $p + \alpha \rightarrow d + {}^3$He at 156 MeV.

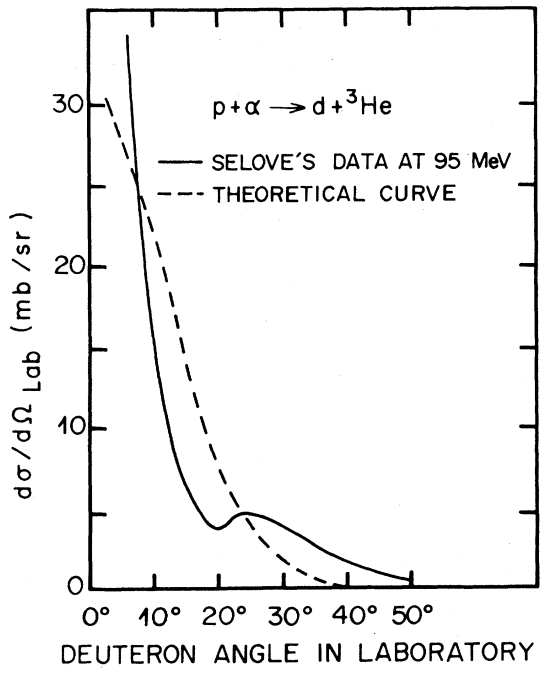

FIG. 4. $d\sigma/d\theta_{d\,\mathrm{lab}}$ for the reaction $p + \alpha \rightarrow d + {}^3$He at 95 MeV.

of the emitted fragment distribution.

To check our conclusion the same formalism is applied to the reaction $p+\alpha$ for which there are several counter results.

Bernas *et al.*[4] and Selove and Teem[5] plotted differential deuteron cross sections versus laboratory emission angle (Figs. 3 and 4). The theoretical curve is obtained by applying the same formalism as before to the reaction $p+\alpha$ (one notices that for two particles in the final state, the energy and the angular distributions in the laboratory are equivalent). The cross section is given by

$$\frac{d\sigma}{dE_d}=\frac{C}{k_0^2}\exp\left[-\frac{1}{3\alpha}(\vec{k}_d-\vec{k}_0)^2\right].$$

An important part of the secondaries can be explained by such a simple approach; this remark, and especially the conclusions drawn from Fig. 2 will allow us to continue the study in such a way.

B. Three-Particle Final State

1. $\alpha+p\rightarrow n+p+{}^3He$ and $p+p+t$

These reactions differ only by Coulomb interactions. If such interactions are neglected the same formulations are applied to calculate cross sections for both reactions. We are interested in energy and not in angular distributions. The Coulomb effects are appreciable only in a certain region of angular distributions. However, they are somewhat smeared out in the energy distribution obtained from the angular distributions by integrating over scattering angles.

As before the interaction between two nucleons (n,p) is considered by the use of the same coordinates and zero-range potential assumption, giving the differential cross section

$$\frac{d\sigma}{dE_{^3\mathrm{He}}}=\frac{C}{k_0^2}\int_0^{\chi_{\max}}\exp\left[-\frac{1}{3\alpha}\left(\vec{k}_{^3\mathrm{He}}-\frac{3\vec{k}_0}{4}\right)^2\right]\chi^2 d\chi.$$

In Fig. 5 the experimental and theoretical distributions normalized to the total number of events are compared. The agreement is not bad even if the number of events is small. In this figure the reactions np^3He and ppt are added.

Innes[6] and Tannenwald[7] measured npt events from neutron induced reactions on helium. If one again neglects the Coulomb forces, it is possible to compare their results with the reaction $p+\alpha \rightarrow n+p+{}^3$He. In that case the cross section is represented as

$$\frac{d\sigma}{dE_{^3\mathrm{He}}}=\frac{C}{k_0^2}\int_0^{\chi_{\max}}\exp\left[-\frac{k_{^3\mathrm{He}}^2}{3\alpha}\right]\chi^2 d\chi.$$

This formula is similar to that given by Ramaty and Lingenfelter[1] with perhaps a somewhat steeper slope for energy distribution. Figures 6 and 7 compare Innes and Tannenwald experimental results with the theoretical calculations. The nor-

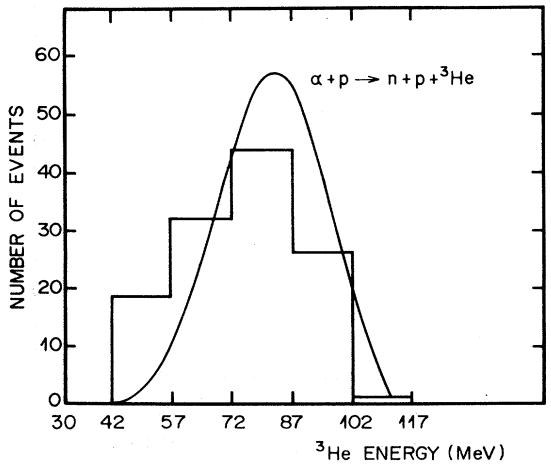

FIG. 5. $d\sigma/dE_{^3\mathrm{He}}$ for the reaction $\alpha+p\rightarrow n+p+{}^3$He experimental and theoretical distributions.

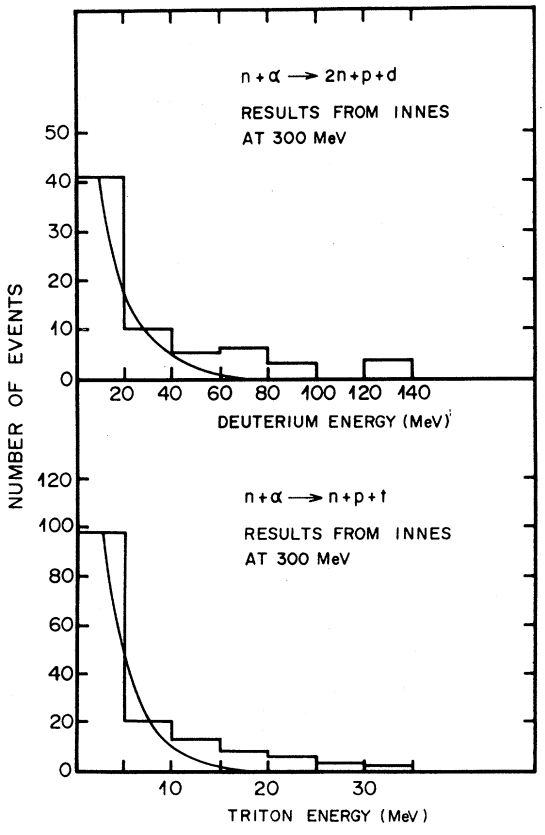

FIG. 6. $d\sigma/dE$ experimental and theoretical distributions for Innes's experiment at 300 MeV.

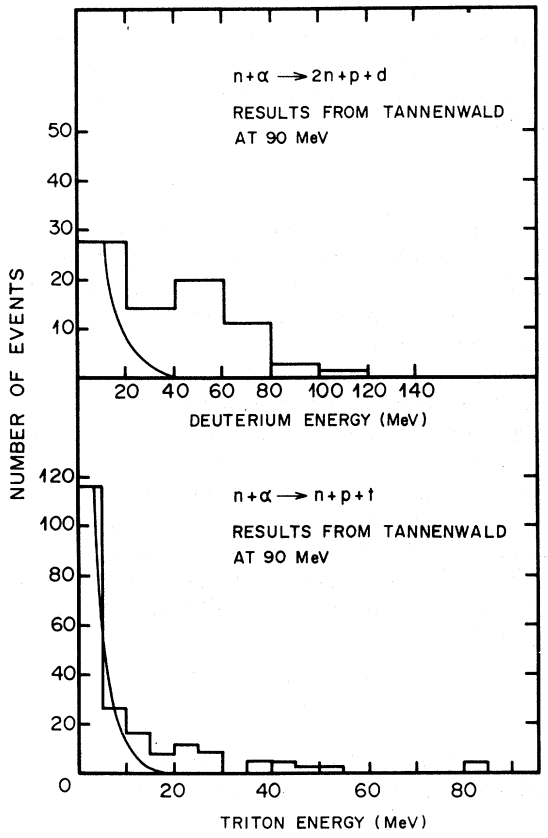

FIG. 7. $d\sigma/dE$ experimental and theoretical distributions for Tannenwald's experiment at 90 MeV.

malization is done for the most populated energy interval. Again from these figures it is possible to conclude that most parts of the spectrum can be explained in this simple way.

2. $\alpha + p \rightarrow p + d + d$

By assuming α-particle breakup, we take the coordinates shown in Fig. 8. By taking the zero-range interaction potential between a nucleon and a deuteron which has the form

$$V(\vec{r}_5 - \vec{r}_d) = V_0 \delta[\vec{r}_5 - \tfrac{1}{2}(\vec{r}_1 + \vec{r}_2)],$$

the differential cross section becomes

$$\frac{d\sigma}{dE_d} = \frac{C}{k_0^2} \int_0^{\chi_{\max}} \exp\left[-\frac{1}{4\alpha}\left(\vec{k}_d - \frac{\vec{k}_0}{2}\right)^2\right] \chi^2 d\chi .$$

Unfortunately, our number of events is too low to compare the experimental data with the calculated results. The only possible test will be a comparison with absolute cross sections (see next paragraph).

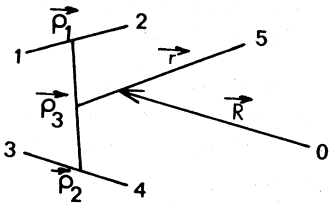

FIG. 8. Coordinate system. Notations are similar to those in Fig. 1.

C. Four-Particle Final State: $\alpha + p \rightarrow n + p + p + d$

Interaction between the proton and two nucleons from helium is considered with the coordinates shown in Fig. 9. For a zero-range potential of the form $V_0\delta[\vec{r}_5 - \frac{1}{2}(\vec{r}_3 + \vec{r}_4)]$, the deuteron cross section becomes

$$\frac{d\sigma}{dE_d} = \frac{C}{k_0^2} \int_0^{\chi_1^{\max}} \int_0^{\chi_2^{\max}} \exp\left(-\frac{\chi_1^2}{2\alpha}\right) \times \exp\left[-\frac{1}{4\alpha}\left(\vec{k}_d - \frac{\vec{k}_0}{2}\right)^2\right] \chi_1^2 \chi_2^2 d\chi_1 d\chi_2$$

if one neglects mass differences between p and n, in which case

$$\vec{\chi}_1 = \tfrac{1}{2}|\vec{k}_3 - \vec{k}_4| .$$

A comparison is only possible with Innes and Tannenwald experiments for which case the cross section has the following form:

$$\frac{d\sigma}{dE_d} = \frac{C}{k_0^2} \int_0^{\chi_1^{\max}} \int_0^{\chi_2^{\max}} \exp\left(-\frac{\chi_1^2}{2\alpha} - \frac{k_d^2}{4\alpha}\right) \chi_1^2 \chi_2^2 d\chi_1 d\chi_2 .$$

Although most of the spectrum is explained for the data of Innes, a different normalization should be chosen to explain Tannenwald's spectrum (Figs. 6 and 7). However, there the number of events is rather poor and we still stay with the above relations.

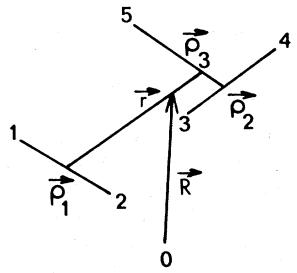

FIG. 9. Coordinate system. Notations are similar to those in Fig. 1.

CROSS-SECTION VARIATION WITH INCIDENT ENERGY

From differential cross sections it is possible to calculate absolute values by an integration over the whole emitted-fragment energy range:

$$\sigma(\epsilon_0) = \int_{\epsilon_1}^{\epsilon_2} \frac{d\sigma(\epsilon_0, \epsilon')}{d\epsilon'} d\epsilon' = C \int_{\epsilon_1}^{\epsilon_2} f(\epsilon_0, \epsilon') d\epsilon',$$

where ϵ_1 and ϵ_2 are limits given by kinematical constraints, ϵ_0 and ϵ the incident and outgoing energies.

A very important point is the estimate of the constant C which should be possible by adjusting the calculated and experimental values. In fact experimental data are given with very large uncertainties and so it is difficult to draw definitive conclusions for C values. Nevertheless we will try to do it and hope that perhaps more experimental results will allow us to get a somewhat better normalization constant C.

Audouze *et al.*[8] and especially Meyer[9] analyzed very closely experimental data from different authors; most times they renormalized them or calculated absolute cross sections from differential values. Their calculations and values from experimentalists are used in the following discussion.

A. $p+\alpha \rightarrow d+{}^3\mathrm{He}$

As our statistics are not too low for this reaction, normalization is done according to our result between 135 and 155 MeV for incident α particles. Error is taken into account and gives both limit curves (Fig. 10[4-7, 10-17]). In this figure Audouze *et al.*'s and Meyer's results are plotted with the addition of directly measured values for $p+\alpha$ and $n+\alpha$ reactions. Our measurement is added versus α energy/nucleon.

For Audouze *et al.*'s results the normalization is quite representative of cross sections except perhaps for Hayakawa *et al.*'s value which is rather high. Nevertheless Meyer's calculations would need a constant about 10% higher to explain his results.

B. $p+\alpha \rightarrow n+p+{}^3\mathrm{He}$ and $p+p+t$ and $p+d+d$

Recent Wilson-chamber measurements from Nicholls *et al.*[10] at 141 MeV have been obtained

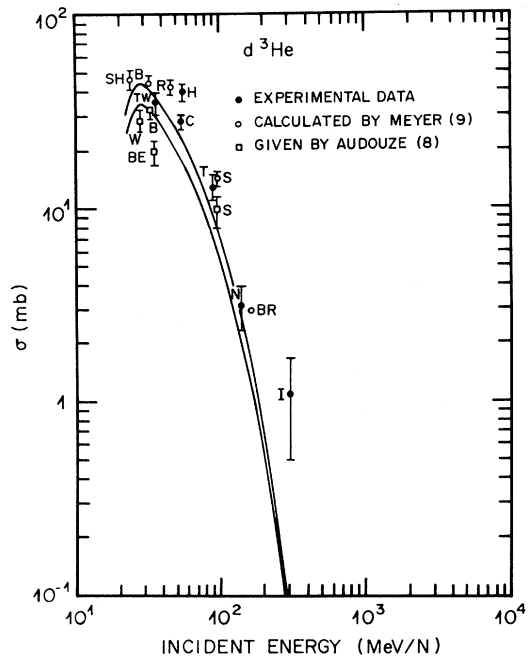

FIG. 10. Variation of $p+\alpha \rightarrow d+{}^3\mathrm{He}$ cross section versus incident energy. The abbreviations are: SH: Shamu and Jenkin (Ref. 11); W: Wickersham (Ref. 14); B: Bunch *et al.* (Ref. 12); BE: Benveniste and Cork (Ref. 13); TW: this work; R: Rogers *et al.* (Ref. 15); C: Cairns *et al.* (Ref. 16); H: Hayakawa *et al.* (Ref. 17); T: Tannenwald (Ref. 7); S: Selove and Teem (Ref. 5); N: Nicholls *et al.* (Ref. 10); BR: Bernas *et al.* (Ref. 4); I: Innes (Ref. 6).

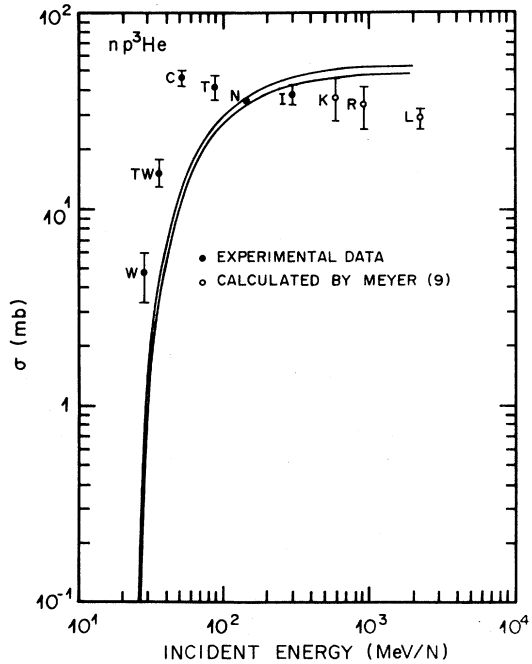

FIG. 11. Variation of $p+\alpha \rightarrow n+p+{}^3\mathrm{He}$ cross section versus incident energy. The abbreviations used are the same as those in Fig. 10 with the addition of : R: Riddiford and Williams (Ref. 19); K: Kozodaev *et al.* (Ref. 20); L: Lebowitz and Miller (Ref. 21).

TABLE I. $\alpha+p$ inelastic cross sections between 135 and 155 MeV.

Reaction	Q value (MeV)	Threshold (MeV)	σ (mb)
$d\,^3$He	−18.4	92	34.9±3.8
ppt	−19.8	99	3.7±1.0
$np\,^3$He	−20.6	103	15.6±2.2
pdd	−23.8	120	1.7±0.6
$nppd$	−26.0	130	0.6±0.6

with a good number of events. Furthermore the comparison they made with the data of Palmieri and Goloskie[18] at 147 MeV for total cross section seems to be quite conclusive. These results are used to try a normalization for the three reactions np^3He, ppt, and pdd.

Experimental and calculated[6,7,10,14,16,19-21] results are plotted in Figs. 11, 12, and 13. At higher energies the agreement is good for np^3He and pdd reactions. It remains also for ppt if one considers Meyer's correction for the Innes result at 300 MeV. The values above 300 MeV certainly include events with emitted π mesons and should give cross sections higher than those predicted

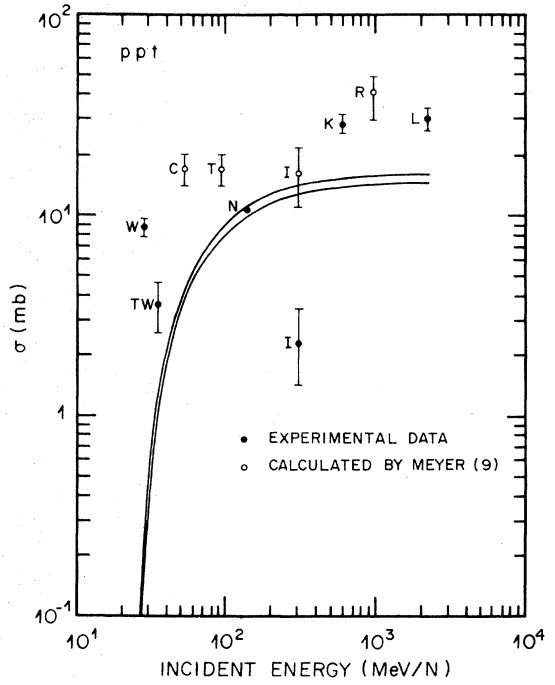

FIG. 12. Variation of $p+\alpha\rightarrow p+p+t$ cross section versus incident energy. Abbreviations are the same as those in Figs. 10 and 11.

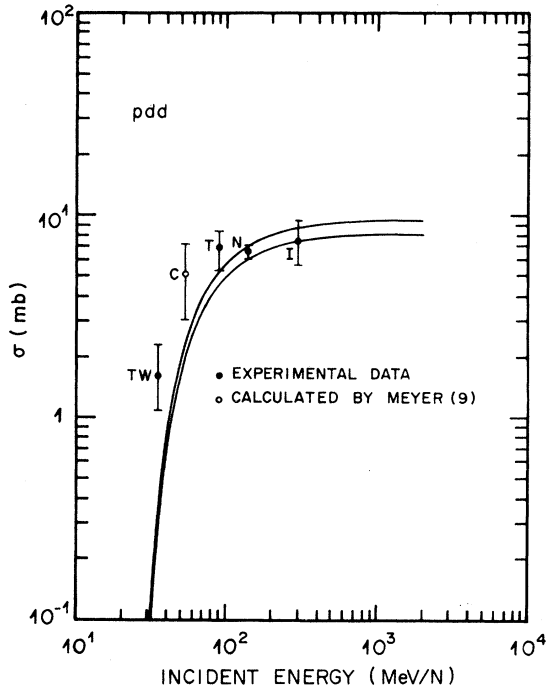

FIG. 13. Variation of $p+\alpha\rightarrow p+d+d$ cross section versus incident energy. Abbreviations are the same as those in Figs. 10 and 11.

by the theory; this is not true for the np^3He channel. In any case Meyer[9] noticed that the results deduced from the experiments of Riddiford and Williams[19] and Kozodaev *et al.*[20] are very uncertain and we are not too concerned about the discrepancy between experiment and theory. At low energy more data around 50 MeV would allow us to draw better conclusions, although errors would be large for low cross sections at such energies.

C. $p+\alpha\rightarrow n+2p+d$

Nicholls *et al.*[10] did not distinguish this reaction from total α-particle breakup so normalization is done according to Innes's result. Only a few data are available for this reaction (Fig. 14) and to draw conclusions about agreement between experiment and theory one has again to consider that the value around 50 MeV is too high.

D. Comment

Meyer[9] studied carefully the variation of total p-α inelastic cross section versus incident energy and found a broad maximum around 50 MeV. If we add all contributions from the theoretical values of inelastic cross sections (except that of

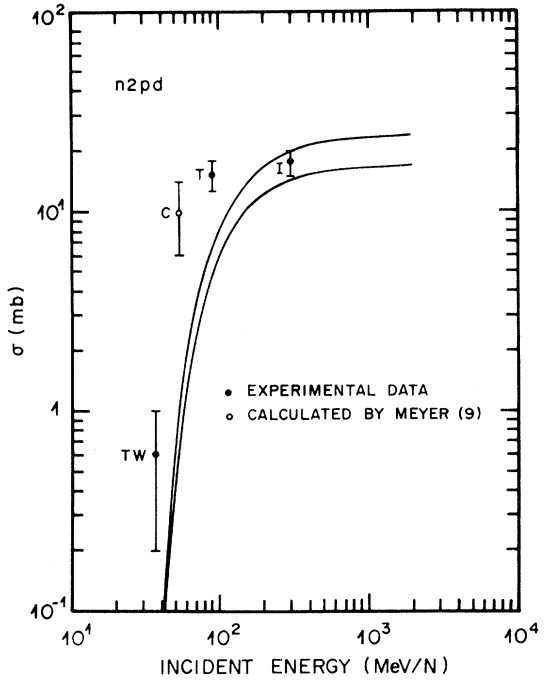

FIG. 14. Variation of $p+\alpha \rightarrow n+2p+d$ cross section versus incident energy. Abbreviations are the same as those in Figs. 10 and 11.

$2n3p$ events we did not study) we obviously do not have such a broad peak. Perhaps one could consider our normalizations too low, but in any case we cannot explain the shape of the experimental distribution. To explain the broad maximum at 50 MeV we would have to introduce strong resonance states, but even if such states exist their contributions would be rapidly smoothed away by phase-space at energies several MeV above the threshold. This is a reason why we emphasize the necessity of doing other cross-section measurements around 50-MeV incident proton energy.

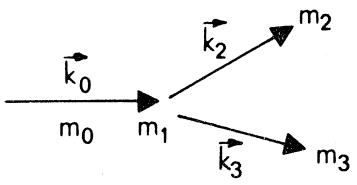

FIG. 15. Kinematics for the two-particle final state. m_i is the mass of particle i; k_i is the momentum of particle i.

CONCLUSION

A simple study of the different production channels for d and ^{3}He fragments in proton-α interactions has been made in order to be applied to cosmic-ray abundance studies. Indeed the proposed differential cross sections explain a rather important part of the emitted fragment-energy spectra and are also simple enough to allow an integration over energy of the contribution of all primaries p and α particles to the secondaries d and ^{3}He energy spectra.

Nevertheless we would like to emphasize that some modifications for the normalization coefficients could be easily done according to some new experimental results of absolute cross sections.

ACKNOWLEDGMENTS

The authors would like to thank Dr. J. Malko for reading the manuscript.

APPENDIX I: TWO PARTICLES IN FINAL STATE

A. Kinematical Constraints (Fig. 15)

$$\cos(\vec{k}_0, \vec{k}_2) = \frac{1}{|\vec{k}_0||\vec{k}_2|}(Ak_0^2 + Bk_2^2 + m_3Q),$$

$$k_{2\,\mathrm{limit}}{}^2 = \frac{k_0^2(1-2AB) - 2m_3BQ \pm \{k_0^2[k_0^2(1-4AB) - 4m_3BQ]\}^{1/2}}{2B^2}.$$

$$A = \frac{1}{2}\left(1 - \frac{m_3}{m_0}\right), \quad B = \frac{1}{2}\left(1 + \frac{m_3}{m_2}\right).$$

B. $\alpha + p \rightarrow (2) + (3)$

$$d\sigma_d = \frac{0.314\times 10^7}{k_0^2} \exp\left[-\frac{1}{3\alpha}\left(\vec{k}_d - \frac{\vec{k}_0}{4}\right)^2\right] dE_d.$$

$$d\sigma_{^3\mathrm{He}} = \frac{0.314\times 10^7}{k_0^2} \exp\left[-\frac{1}{3\alpha}\left(\vec{k}_{^3\mathrm{He}} - \tfrac{3}{4}\vec{k}_0\right)^2\right] dE_{^3\mathrm{He}}.$$

C. $p+\alpha \rightarrow (2)+(3)$

$$d\sigma_d = \frac{0.788\times 10^6}{k_0^2} \exp\left[-\frac{1}{3\alpha}(\vec{k}_d - \vec{k}_0)^2\right] dE_d .$$

$$d\sigma_{^3\mathrm{He}} = \frac{0.788\times 10^6}{k_0^2} \exp\left[-\frac{1}{3\alpha} k_{^3\mathrm{He}}^2\right] dE_{^3\mathrm{He}} .$$

APPENDIX II: THREE PARTICLES IN FINAL STATE

A. Kinematical Constraints (Fig. 16)

$$\cos(\vec{k}_0, \vec{k}_2) = \frac{1}{|\vec{k}_0||\vec{k}_2|}\left[Ak_0^2 + Bk_2^2 + C\chi^2 + MQ\right],$$

$$k_{2\,\mathrm{limit}}^2 = \frac{k_0^2(1-2AB) - 2BC\chi^2 - 2MBQ \pm \left[k_0^2\left|k_0^2(1-4AB) - 4BC\chi^2 - 4MBQ\right|\right]^{1/2}}{2B^2},$$

with

$$0 \leqslant \chi^2 \leqslant \frac{k_0^2(1-4AB) - 4MBQ}{4BC} .$$

$$M = m_3 + m_4, \quad A = \frac{1}{2}\left[1 - \frac{M}{m_0}\right], \quad B = \frac{1}{2}\left[1 + \frac{M}{m_2}\right], \quad \mu = \frac{m_3 m_4}{m_3 + m_4}, \quad C = \frac{M}{2\mu}, \quad \vec{\chi} = \frac{m_4\vec{k}_3 - m_3\vec{k}_4}{M} .$$

B. $\alpha + p \rightarrow n + p + {}^3\mathrm{He}$ or $p + p + t$

$$d\sigma_2 = \frac{C}{k_0^2}\int_0^{\chi_{\max}} \exp\left[-\frac{1}{3\alpha}(\vec{k}_2 - \tfrac{3}{4}\vec{k}_0)^2\right]\chi^2\, d\chi\, dE_2 .$$

$C_{^3\mathrm{He}} = 0.228\times 10^1$ and $C_t = 0.678$.

C. $p + \alpha \rightarrow n + p + {}^3\mathrm{He}$ or $p + p + t$

$$d\sigma_2 = \frac{C}{k_0^2}\int_0^{\chi_{\max}} e^{-k_2^2/3\alpha}\chi^2 d\chi\, dE_2 .$$

$C_{^3\mathrm{He}} = 0.592$ and $C_t = 0.176$.

D. $\alpha + p \rightarrow p + d + d$

$$d\sigma_d = \frac{0.146}{k_0^2}\int_0^{\chi_{\max}} \exp\left[-\frac{1}{4\alpha}\left(\vec{k}_d - \frac{\vec{k}_0}{2}\right)^2\right]\chi^2 d\chi\, dE_d .$$

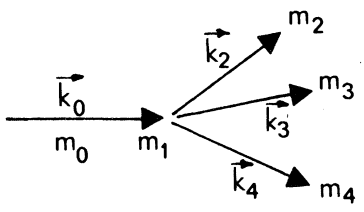

FIG. 16. Kinematics for three-particle final-state. Notations are the same as in Fig. 15.

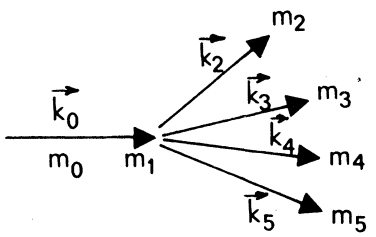

FIG. 17. Kinematics for four-particle final-state. Notations are the same as in Fig. 15.

E. $p+\alpha \rightarrow p+d+d$

$$d\sigma_d = \frac{0.377\times 10^{-1}}{k_0^{\,2}} \int_0^{\chi_{\max}} \exp\left(-\frac{k_d^{\,2}}{4\alpha}\right) \chi^2 d\chi\, dE_d\,.$$

APPENDIX III: FOUR PARTICLES IN FINAL STATE

A. Kinematical Constraints (Fig. 17)

$$\cos(\vec{k}_0, \vec{k}_2) = \frac{1}{|\vec{k}_0||\vec{k}_2|}\left(Ak_0^{\,2} + Bk_2^{\,2} + C\chi_1^{\,2} + D\chi_2^{\,2} + M_2 Q\right),$$

$$k_{2\,\text{limit}}^{\,2} = \frac{k_0^{\,2}(1-2AB) - 2BC\chi_1^{\,2} - 2BD\chi_2^{\,2} - 2M_2BQ \pm \delta}{2B^2},$$

with

$$\delta^2 = k_0^{\,2}\left[k_0^{\,2}(1-4AB) - 4BC\chi_1^{\,2} - 4BD\chi_2^{\,2} - 4M_2BQ\right]$$

and

$$0 \leqslant C\chi_1^{\,2} + D\chi_2^{\,2} \leqslant \frac{k_0^{\,2}(1-4AB) - 4M_2BQ}{4B}.$$

$$M_1 = m_3 + m_4, \quad M_2 = m_3 + m_4 + m_5, \quad \vec{\chi}_1 = \frac{m_4\vec{k}_3 - m_3\vec{k}_4}{M_1}, \quad \vec{\chi}_2 = \frac{M_1\vec{k}_5 - m_5(\vec{k}_3+\vec{k}_4)}{M_2},$$

$$A = \frac{1}{2}\left(1 - \frac{M_2}{m_0}\right), \quad B = \frac{1}{2}\left(1 + \frac{M_2}{m_2}\right), \quad C = \frac{1}{2}\left(\frac{M_2}{m_3} + \frac{M_2}{m_4}\right), \quad D = \frac{1}{2}\left(\frac{M_2}{M_1} + \frac{M_2}{m_5}\right).$$

B. $\alpha + p \rightarrow n + 2p + d$

$$d\sigma_d = \frac{0.634\times 10^{-6}}{k_0^{\,2}} \int_0^{\chi_1^{\max}} \int_0^{\chi_2^{\max}} e^{-\chi_1^{\,2}/2\alpha} \exp\left[-\frac{1}{4\alpha}\left(\vec{k}_d - \frac{\vec{k}_0}{2}\right)^2\right] \chi_1^{\,2}\chi_2^{\,2} d\chi_1 d\chi_2 dE_d\,.$$

C. $p + \alpha \rightarrow n + 2p + d$

$$d\sigma_d = \frac{0.163\times 10^{-6}}{k_0^{\,2}} \int_0^{\chi_1^{\max}} \int_0^{\chi_2^{\max}} e^{-\chi_1^{\,2}/2\alpha}\, e^{-k_d^{\,2}/4\alpha}\, \chi_1^{\,2}\chi_2^{\,2} d\chi_1 d\chi_2 dE_d\,.$$

To get cross sections in mb all momenta have to be expressed in (MeV/c). Here we took

$$Q = \sum_{f=2}^{n} m_f - m_1 - m_0\,.$$

[1] R. Ramaty and R. E. Lingenfelter, Goddard Space Flight Center Report No. X-611-68-144, 1968 (unpublished).
[2] M. Jung *et al.*, Phys. Rev. C **5**, 579 (1972).
[3] H. Collard *et al.*, Phys. Rev. **138**, B57 (1965).
[4] M. Bernas *et al.*, Nucl. Phys. **A156**, 289 (1970).
[5] W. Selove and S. M. Teem, Phys. Rev. **112**, 1654 (1958).
[6] W. H. Innes, UCRL Report No. UCRL 80-40, 1957 (unpublished).
[7] P. E. Tannenwald, Phys. Rev. **89**, 508 (1953).
[8] J. Audouze *et al.*, *High Energy Nuclear Reactions in Astrophysics* (Benjamin, New York, 1967).
[9] J. P. Meyer, Astron. Astrophys. (to be published).
[10] J. E. Nicholls *et al.*, Nucl. Phys. **A181**, 329 (1972).
[11] R. E. Shamu and J. G. Jenkin, Phys. Rev. **135**, B99 (1964).
[12] S. M. Bunch *et al.* Nucl. Phys. **53**, 341 (1964).
[13] J. Benveniste and B. Cork, Phys. Rev. **89**, 422 (1953).
[14] A. F. Wickersham, Phys. Rev. **107**, 1050 (1957).
[15] J. G. Rogers *et al.*, Phys. Rev. C **2**, 827 (1970).
[16] D. J. Cairns *et al.*, Nucl. Phys. **60**, 369 (1964).
[17] S. Hayakawa *et al.*, Phys. Lett. **8**, 330 (1964).
[18] J. W. Palmieri and R. G. Goloskie, Nucl. Phys. **59**, 253 (1964).
[19] L. Riddiford and A. W. Williams, Proc. R. Soc. **A257**, 316 (1960).
[20] M. S. Kozodaev *et al.*, [Soy. Phys.-JETP **38**, 511 (1960)].
[21] E. Lebowitz and J. M. Miller, Phys. Rev. **177**, 1548 (1969).